

Cross sections for the $^{35}\text{Cl}(n, \alpha)^{32}\text{P}$ reaction in the 3.3–5.3 MeV neutron energy region

E. Sansarbayar^{1,2,*}, Yu. M. Gledenov¹, I. Chuprakov^{1,3,4}, G. Khuukhenkhoo^{1,2}, G. S. Ahmadov^{1,5},
L. Krupa^{6,7}, Guohui Zhang⁸, Haoyu Jiang⁸, Zengqi Cui⁸, Yiwei Hu⁸, Jie Liu⁸, N. Battsooj²,
I. Wilhelm⁷, M. Solar⁷, R. Sykora⁷ and Z. Kohout⁷

¹Frank Laboratory of Neutron Physics, Joint Institute for Nuclear Research, Dubna 141980, Russia

²Nuclear Research Center, National University of Mongolia, Ulaanbaatar 210646, Mongolia

³L.N. Gumilyov Eurasian National University, Nur-sultan 010000, Kazakhstan

⁴The Institute of Nuclear Physics, Ministry of Energy of the Republic of Kazakhstan, Almaty 050032, Kazakhstan

⁵National Nuclear Research Centre, Baku AZ1073, Azerbaijan

⁶Flerov Laboratory of Nuclear Reactions, Joint Institute for Nuclear Research, Dubna 141980, Russia

⁷Institute of Experimental and Applied Physics, Czech Technical University in Prague, Husova 240/5, Prague 1, 110 00 Czech Republic

⁸State Key Laboratory of Nuclear Physics and Technology, Institute of Heavy Ion Physics,
School of Physics, Peking University, Beijing 100871, China



(Received 22 July 2021; accepted 14 October 2021; published 25 October 2021)

Cross sections for the $^{35}\text{Cl}(n, \alpha)^{32}\text{P}$ reaction were systematically measured at incident neutron energies in the range of 3.3 to 5.3 MeV. The experiment was carried out on the Van de Graaff accelerator EG-5 at the Frank Laboratory of Neutron Physics, Joint Institute for Nuclear Research, Russia. Fast neutrons were produced in the reaction $^2\text{H}(d, n)^3\text{He}$. Alpha particles from the (n, α) reactions were detected using a gridded ionization chamber (GIC) in which various ^{35}Cl samples (NaCl and BaCl₂, on a tantalum backing) were placed back to back. The relative and absolute neutron fluxes were measured by two samples of $^{238}\text{U}_3\text{O}_8$ (99.999%) inside the GIC. Data obtained in this measurement were compared with other experimental data of the existing library and theoretical calculations by the TALYS code. Presented data for the $^{35}\text{Cl}(n, \alpha)^{32}\text{P}$ reaction should help to clarify discrepancies in the various published nuclear data.

DOI: [10.1103/PhysRevC.104.044620](https://doi.org/10.1103/PhysRevC.104.044620)

I. INTRODUCTION

As a widespread element in nature, chlorine is one of the chemical elements necessary for humans. $^{35}\text{Cl}(n, \alpha)^{32}\text{P}$ is one of the main reaction channels for the neutron-induced chlorine reaction since the ^{35}Cl abundance is 75.77%. Experimental study of this reaction can improve the existing library of nuclear data and can be used to test appropriate nuclear reaction models. The cross sections for the $^{35}\text{Cl}(n, \alpha)^{32}\text{P}$ reaction are useful for nuclear technology applications. They were used to estimate fast neutron flux from the JCO criticality accident in 1999 [1]. The beta radioactive product ^{32}P can be used to study the absorption of phosphate fertilizers by plants using the radionuclide tracking method. In addition, chloride is a component of the coolant in the molten salt reactor, which is one of the six most promising GEN-IV reactors [2]. For the $^{35}\text{Cl}(n, \alpha)^{32}\text{P}$ reaction, eight measurements [3–9] in the neutron energy range of 1–4 MeV, five measurements [10–14] close to 14 MeV region can be found in the EXFOR library [15]. These experimental data agree well with nuclear evaluation data libraries [15–19] between 2 to 4 MeV and around 14 MeV, with the exception of JENDL-4.0 [20].

Investigations using the activation method were performed in the neutron energy range 0.1–2 MeV and experimental results have a big difference with all nuclear data libraries [16–20]. The studies were performed with an ionization chamber at the neutron energy of 3 MeV [4], where the neutron flux was monitored with the $^{14}\text{N}(n, \alpha)^{11}\text{B}$ reaction. The error of the total cross-section measurements was estimated 100% for the reaction $^{35}\text{Cl}(n, \alpha)^{32}\text{P}$. The $^{35}\text{Cl}(n, \alpha)^{32}\text{P}$ reaction was also studied in a narrow energy range of 2.42–2.74 MeV [9]. In Ref. [21] the cross section of the reaction channels α_0 , α_1 was measured in the energy range of 2.75–5.75 MeV and $\alpha_{3,4}$ was measured at 5.75 MeV only. The total cross-section of the reaction $^{35}\text{Cl}(n, \alpha)^{32}\text{P}$ was not obtained in Ref. [21]. This work is devoted to measuring the cross sections for the $^{35}\text{Cl}(n, \alpha)^{32}\text{P}$ reaction in the 3.3–5.3 MeV region. In our measurements, we used gridded ionization chamber (GIC) and three (pairs of double-sided) samples of NaCl and BaCl₂. The cross sections for the $^{35}\text{Cl}(n, \alpha)^{32}\text{P}$ reaction were measured with high accuracy at incident neutron energies of 3.3, 3.9, 4.3, 4.8, 5.0, 5.1, and 5.3 MeV. Our experimental data are compared with the TALYS [22,23] calculations and existing experimental and evaluation data. In addition, the alpha-clustering factor was for the first time obtained using the knock-on model for the $^{35}\text{Cl}(n, \alpha)^{32}\text{P}$ reaction at the different neutron energies.

* sansar@nf.jinr.ru

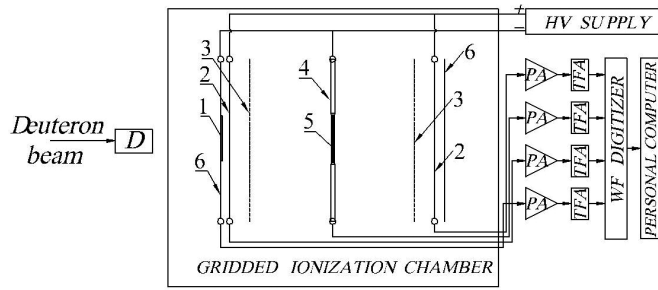


FIG. 1. Scheme of the experimental setup. 1- ^{238}U sample of fission chamber; 2,3,4-anode, grid, and cathode of the GIC, respectively; 5-samples on the sample changer; 6-Fission chamber cathode; PA-charge sensitive preamplifier; TFA-timing filter amplifier.

II. EXPERIMENTAL DETAILS

A. Neutron source

The experiments were carried out on the Van de Graaff accelerator EG-5 at the Frank Laboratory of Neutron Physics, Joint Institute for Nuclear Research (FLNP, JINR). A simplified block diagram of the experimental setup is shown in Fig. 1. Fast neutrons were produced via the $^2\text{H}(d, n)^3\text{He}$ reaction using the deuterium gas target 2.0 cm long and 1 cm in diameter. The cell with deuterium gas was separated from the vacuum in the beam channel by molybdenum foil with a thickness of $6.0\ \mu\text{m}$. The incident deuteron beam current was approximately $2.0\ \mu\text{A}$, and the pressure of gaseous deuterium during the measurement was 2.5 atm.

B. Samples

Natural NaCl and BaCl₂ with high chemical purity ($\geq 99.5\%$) were used as sample materials. They were prepared using the vacuum evaporation method on a tantalum backing 0.1 mm thick and 48 mm in diameter. The thicknesses of the NaCl samples were 707, 667, 302, and $289\ \mu\text{g}/\text{cm}^2$, while for BaCl₂ these values were 125 and $108\ \mu\text{g}/\text{cm}^2$. The diameter of all samples was 44 mm. Two samples of $^{238}\text{U}_3\text{O}_8$ (99.999%, $N_{\text{U}} = 1.74 \times 10^{19}$, and $N_{\text{U}} = 1.5 \times 10^{19}$ which were placed on the sample changer and the fission cathode, respectively) were

used to measure absolute and relative neutron flux. An alpha source containing the ^{234}U and ^{238}U isotopes was used for energy calibration of the detection system.

C. Detectors and data acquisition

The GIC with almost 100% detection efficiency was developed at the FLNP, JINR. The structure of the GIC and its characteristics were in more detail presented in Ref. [24]. One of the $^{238}\text{U}_3\text{O}_8$ samples was glued to one of the GIC shields to monitor the relative neutron flux. Thus, the shielding electrode was used as the fission cathode of the fission chamber. Moreover, a ^3He long counter was also used as a neutron flux monitor in all measurements. The working gas of the GIC was Kr + 3% CH₄, and the pressure was 0.6 atm, so the alpha particles could stop before reaching the grids. The lower gas pressure reduces the proton signal pulse height from the $^{35}\text{Cl}(n, p)$ reaction and the background from the working gas. The grid electrodes were grounded, while high voltages of -1200 and $800\ \text{V}$ were applied to the cathodes and anodes, respectively. Two samples of BaCl₂ and NaCl on tantalum backing foils were placed back to back on the GIC cathode. The detector signals were obtained using a 14-bit Pixie-16 module with a sampling frequency of 250 MHz. The Pixie system consists of a chassis (PXI6023-XIA 14, Wiener), an embedded controller (NI PXI-8820), and a high-speed digitizer (Pixie-16).

D. Simulation

Before measurements, we performed calculations to predict the experimental spectra of the $^{35}\text{Cl}(n, \alpha)^{32}\text{P}$ reaction and possible interference reactions, including (n, p) , (n, α) reactions of Kr, ^{37}Cl , O (leaking from air -0.05%), N (leaking from air -0.1%), Na, Ba, $^1\text{H}(n, p)$, and the (n, p) reaction of ^{35}Cl . Simulations were carried out for solid samples of the NaCl and BaCl₂ with a thickness of 700, 300, and $100\ \mu\text{g}/\text{cm}^2$ in the range of incident neutron energy of 4–6 MeV. Figure 2 shows the calculated energy spectra of α particles from the $^{35}\text{Cl}(n, \alpha)^{32}\text{P}$ reaction at $E_n = 5.0\ \text{MeV}$, where α particles from the sample move forward [Fig. 2(a)] and backward [Fig. 2(b)] with respect to the neutron beam.

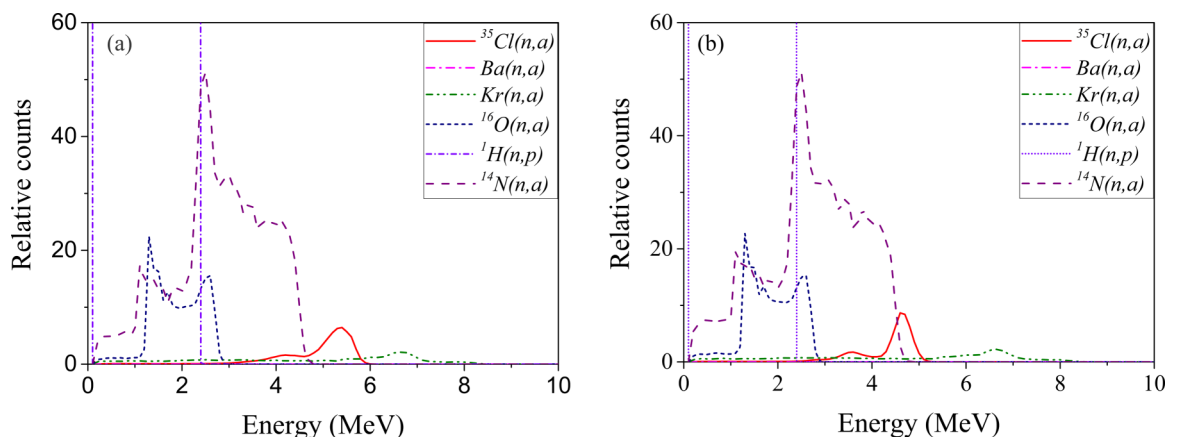


FIG. 2. Calculated energy spectra of α particles from the reaction $^{35}\text{Cl}(n, \alpha)^{32}\text{P}$ at $E_n = 5.0\ \text{MeV}$ (a) forward and (b) backward directions.

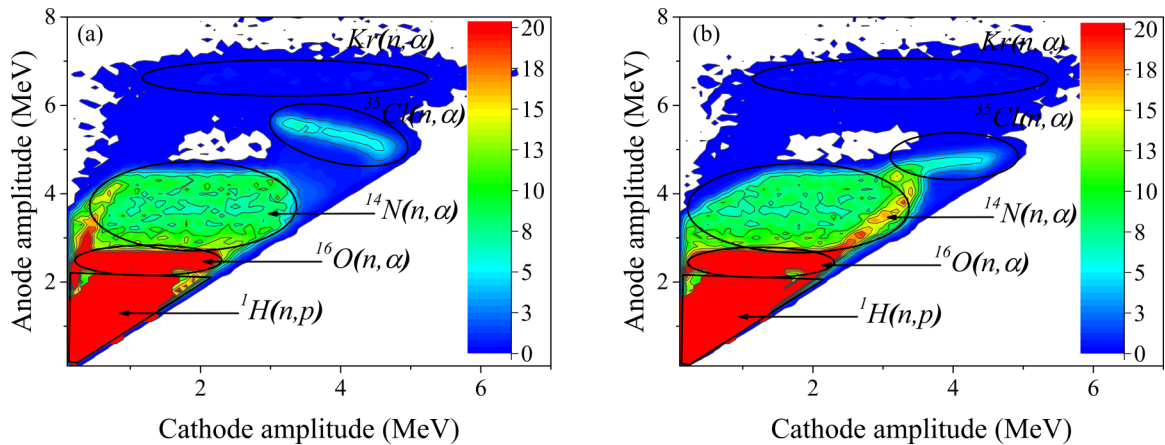


FIG. 3. Two-dimensional calculated cathode-anode spectra of α particles from the reaction $^{35}\text{Cl}(n, \alpha) ^{32}\text{P}$ at $E_n = 5.0$ MeV, (a) forward and (b) backward directions with the contribution of background reactions.

Here the effects of background reactions are also indicated. Self-absorption correction for α particles was taken into account for the determination of the GIC efficiency. The two-dimensional calculated cathode-anode spectra are shown in Figs. 3 and 4.

It was seen that the $^{14}\text{N}(n, \alpha)$ and $^{16}\text{O}(n, \alpha)$ reactions from working gas were the main source of the background, especially for the backward measurement of the $^{35}\text{Cl}(n, \alpha)$ reaction. The background from ^{37}Cl is very low. Alpha particles emitted from the $^{35}\text{Cl}(n, \alpha) ^{32}\text{P}$ reaction were simulated for various components and thicknesses of the samples using the Monte Carlo method to determine the detection efficiency of alpha particles. The detection efficiency of alpha particles was determined 80%–97% depending on the neutron energy, sample thickness, and thresholds of measurements.

III. EXPERIMENTAL DATA

A. Experimental procedure

The experiments were carried out at the six neutron energies of the 3.3–5.3 MeV range. At each energy point, the

following five measurement runs were performed: energy calibration of the experimental setup using two groups of alpha particles of 4.197 and 4.775 MeV energy emitted by the mixed alpha source (^{234}U and ^{238}U); measurements with the back-to-back ^{35}Cl samples (foreground); measurement with the back-to-back Ta backings (background); calibration of absolute neutron flux using the $^{238}\text{U}(n, f)$; and recalibration of the experimental setup to check its stability. The signals from the fission fragments of the fission chamber were fed into the data acquisition system when measuring the foreground, background, and $^{238}\text{U}(n, f)$ reaction. In all measurements, a ^3He long counter was also used as a neutron flux monitor. Since the analysis of the data showed that the results of monitoring the neutron beam using the long counter and the fission chamber are very close, further in the article we use the data from the fission chamber.

B. Determination of the fission events using the $^{238}\text{U}_3\text{O}_8$ sample

To determine the absolute neutron flux, the total fission counts of the $^{238}\text{U}_3\text{O}_8$ sample were used. A typical anode spectrum of fission fragments is shown in Fig. 5 as an example.

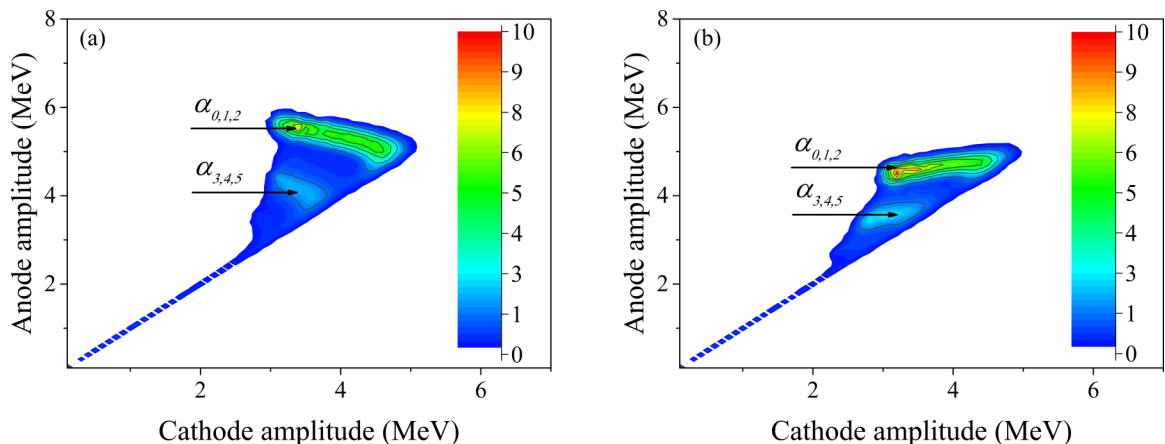


FIG. 4. Background-subtracted two-dimensional calculated cathode-anode spectra of α particles from the reaction $^{35}\text{Cl}(n, \alpha) ^{32}\text{P}$ at $E_n = 5.0$ MeV, (a) forward and (b) backward directions.

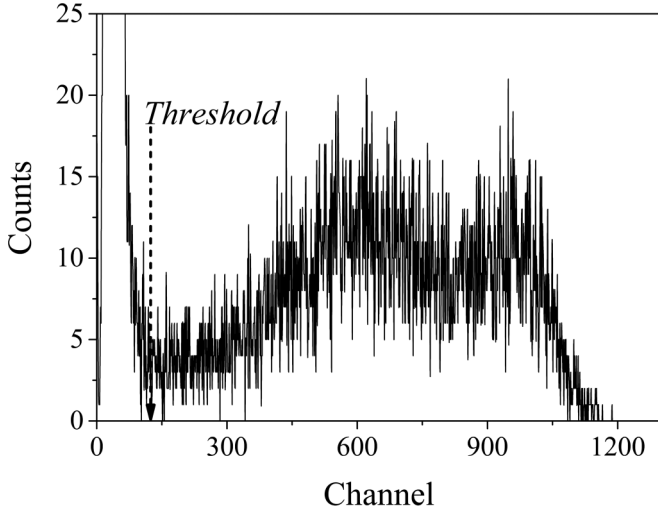


FIG. 5. The anode spectrum of fission fragments for measuring the absolute neutron flux of the $^{238}\text{U}(n, f)$ reaction at $E_n = 5.0$ MeV.

To obtain the total number of fission, it is necessary to determine the detection efficiency ϵ_f of the GIC for fission counts which can be obtained by the expression [25]

$$\epsilon_f = 1 - \frac{\tau}{2(R_{\max} - R_{\text{threshold}})}, \quad (1)$$

where τ is the thickness of the sample, R_{\max} is the maximum stopping range of fission fragments, and $R_{\text{threshold}}$ is the threshold value of a fission fragment. The SRIM code [26] was used to obtain the parameters of Eq. (1). The detection efficiency of the GIC for the fission fragments was about 97% in this work. The relative neutron flux can be determined as mentioned in Sec. II B, using the fission counts from the $^{238}\text{U}_3\text{O}_8$ sample glued on the fission cathode for each experimental step.

C. Alpha events from the $^{35}\text{Cl}(n, \alpha)^{32}\text{P}$ reaction

Two-dimensional cathode-anode spectra of the $^{35}\text{Cl}(n, \alpha)^{32}\text{P}$ reaction have been analyzed. Figure 6 shows the two-dimensional spectra for the $^{35}\text{Cl}(n, \alpha)^{32}\text{P}$ reaction after background subtraction at $E_n = 5.3$ MeV in the

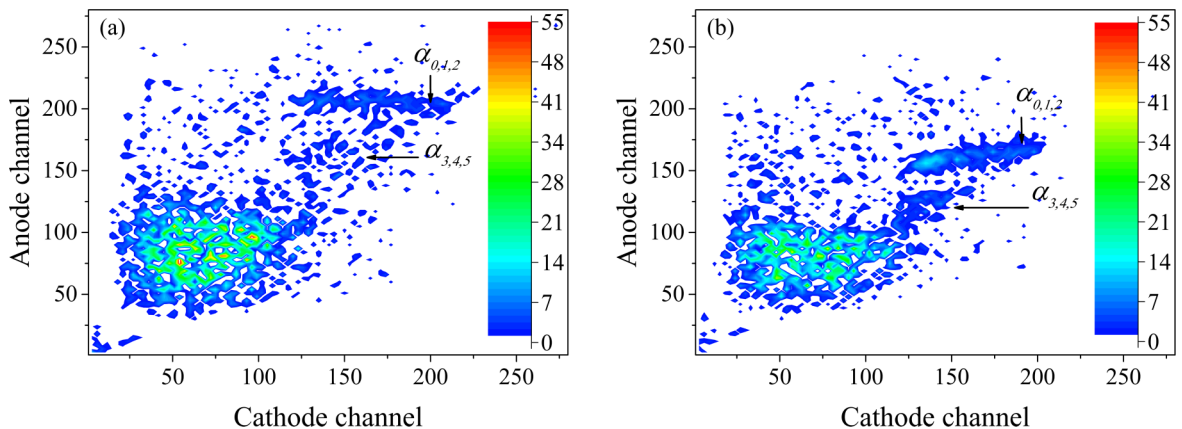


FIG. 6. Background subtracted two-dimensional spectra of the $^{35}\text{Cl}(n, \alpha)^{32}\text{P}$ reaction in the (a) forward and (b) backward directions at $E_n = 5.3$ MeV.

TABLE I. Sources of the uncertainty.

Source	Magnitude (%)
$N_{^{238}\text{U}}$	2.0 ^a
$N_{^{35}\text{Cl}}$	3.0 ^a
$\sigma_{n,f}$	0.7 ^a
Fis_f	3.0 ^a
Fis_α	3.0 ^a
N_α	5.0–11.0 ^a
N_f	3.0 ^a
σ_α	4.8–11.0 ^b

^aFor the forward and backward cross sections.

^bFor the total cross sections.

forward and backward directions. Background counts were normalized using the fission counts from the $^{238}\text{U}_3\text{O}_8$ sample glued on the fission cathode. After background subtraction, the two-dimensional spectrum was projected onto the anode channel (see Fig. 7). Thresholds were set to separate the effective events from the background events that cannot be subtracted. The number of pure α events within the threshold values N_α can be determined as follows:

$$N_\alpha = N_\alpha^{\text{foreground}} - CN_\alpha^{\text{background}}, \quad (2)$$

where $N_\alpha^{\text{foreground}}$ and $N_\alpha^{\text{background}}$ are the total numbers of counts within the threshold values of the foreground and background measurements, respectively. C is the background normalization factor, which is determined by the ratio of events from $^{238}\text{U}_3\text{O}_8$ during the foreground and background measurements.

D. Determination of the cross sections

The cross section $\sigma_{n,\alpha}$ of the $^{35}\text{Cl}(n, \alpha)^{32}\text{P}$ reaction was obtained using the following formula:

$$\sigma_{n,\alpha} = K \sigma_{n,f} \frac{N_\alpha \epsilon_f N_{^{238}\text{U}}}{N_f \epsilon_\alpha N_{^{35}\text{Cl}}}, \quad (3)$$

where $K = \frac{Fis_f}{Fis_\alpha}$, Fis_α and Fis_f are fission-fragment counts of the fission chamber while the $^{35}\text{Cl}(n, \alpha)^{32}\text{P}$ and $^{238}\text{U}(n, f)$

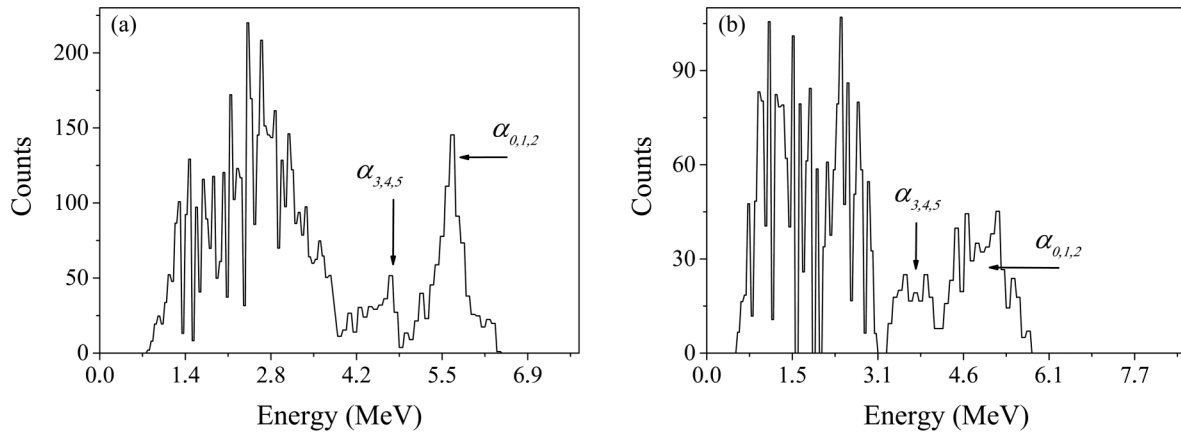


FIG. 7. The anode projection spectra of net events of the reaction $^{35}\text{Cl}(n, \alpha)^{32}\text{P}$ in the (a) forward and (b) backward directions at $E_n = 5.3$ MeV.

reactions were measured, respectively. $\sigma_{n,f}$ is the $^{238}\text{U}(n, f)$ reactions cross section taken from ENDF/B-VIII [16]. N_α and N_f are the numbers of pure alpha and fission events within the threshold value in the $^{35}\text{Cl}(n, \alpha)^{32}\text{P}$ and $^{238}\text{U}(n, f)$ reactions. ϵ_f and ϵ_α are detection efficiencies of the fission and alpha events. $N_{^{238}\text{U}}$ and $N_{^{35}\text{Cl}}$ are the atom numbers of the ^{238}U and ^{35}Cl , respectively.

IV. RESULTS AND DISCUSSIONS

A. Experimental cross sections of the $^{35}\text{Cl}(n, \alpha)^{32}\text{P}$ reaction

Forward and backward cross sections of the reaction $^{35}\text{Cl}(n, \alpha)^{32}\text{P}$ were obtained by the formula (3). The

cross-section uncertainties at six energies were calculated by adding uncertainties listed in Table I. Uncertainty of the total $^{35}\text{Cl}(n, \alpha)^{32}\text{P}$ cross section was in the range of 4.0% to 6.3%. Similarly, the cross-section uncertainties of $^{35}\text{Cl}(n, \alpha_{0,1,2})^{32}\text{P}$ and $^{35}\text{Cl}(n, \alpha_{3,4,5})^{32}\text{P}$ were obtained to be 7.9%–11.0% and 10.2%–12.0%, respectively. The total (n, α) cross section can be obtained by summing the forward and the backward cross sections. The results are shown in Table II and Fig. 8. Obtained cross sections of $^{35}\text{Cl}(n, \alpha)^{32}\text{P}$ were compared with other results, nuclear data libraries, and calculation results by TALYS-1.9. Figure 8 shows that our experimental cross sections for the $^{35}\text{Cl}(n, \alpha)^{32}\text{P}$ reaction are in agreement with evaluated data by the ENDF/B-VIII.0, FENDL-3.1c,

TABLE II. Measured (n, α) cross sections for ^{35}Cl .

Energy (MeV)	Samples (thickness, $\mu\text{g}/\text{cm}^2$)	Cross sections (mbarn)				
		Forward	Backward	Total		TALYS-1.9
				Experiment		
3.3	NaCl(302, ^a 289 ^b)	24.2 ± 3.4	19.4 ± 3.0	43.6 ± 4.5	43.6 ± 4.5	24
3.9	NaCl(302, ^a 289 ^b)	28.6 ± 3.0	26.9 ± 2.5	55.5 ± 3.9	55.5 ± 3.9	57.4
4.3	NaCl(707, ^a 667 ^b)	35.7 ± 3.7	37.6 ± 3.9	73.3 ± 5.4		
		38.6 ± 4.0	36.7 ± 3.8	75.3 ± 5.5		
	NaCl(302, ^a 289 ^b)	40.3 ± 4.2	36.3 ± 3.8	76.6 ± 5.6	74.3 ± 2.8	79.9
	BaCl ₂ (125, ^a 108 ^b)	38.0 ± 3.5	32.7 ± 3.0	70.7 ± 4.6		
4.5	NaCl(302, ^a 289 ^b)	40.5 ± 6.8	35.1 ± 6.0	75.6 ± 9.0		
	NaCl(302, ^a 289 ^b)	47.9 ± 4.4	38.4 ± 3.5	86.3 ± 5.6	86.9 ± 5.5	87.7
4.8	BaCl ₂ (125, ^a 108 ^b)	44.2 ± 6.3	43.3 ± 7.3	87.5 ± 9.6		
	NaCl(302, ^a 289 ^b)	57.3 ± 5.2	44.7 ± 4.0	102.0 ± 6.5	101.0 ± 5.1	100.9
5.0	BaCl ₂ (125, ^a 108 ^b)	48.3 ± 4.7	52.3 ± 6.5	100.6 ± 8.0		
	NaCl(302, ^a 289 ^b)	58.1 ± 4.7	43.4 ± 4.5	101.5 ± 6.5	100.3 ± 4.2	108
5.1	NaCl(707, ^a 667 ^b)	52.4 ± 3.6	46.7 ± 4.2	99.1 ± 5.5		
	NaCl(302, ^a 289 ^b)	61.8 ± 6.2	45.4 ± 4.5	107.2 ± 7.7	105.4 ± 5.8	110.1
5.3	BaCl ₂ (125, ^a 108 ^b)	53.3 ± 5.9	50.4 ± 6.6	103.7 ± 8.8		
	NaCl(302, ^a 289 ^b)	59.6 ± 5.4	46.6 ± 4.3	106.2 ± 6.9	116.4 ± 5.2	114.8
	BaCl ₂ (125, ^a 108 ^b)	60.5 ± 5.0	66.1 ± 6.1	126.6 ± 7.9		

^aFor the forward cross sections.

^bFor the backward cross sections.

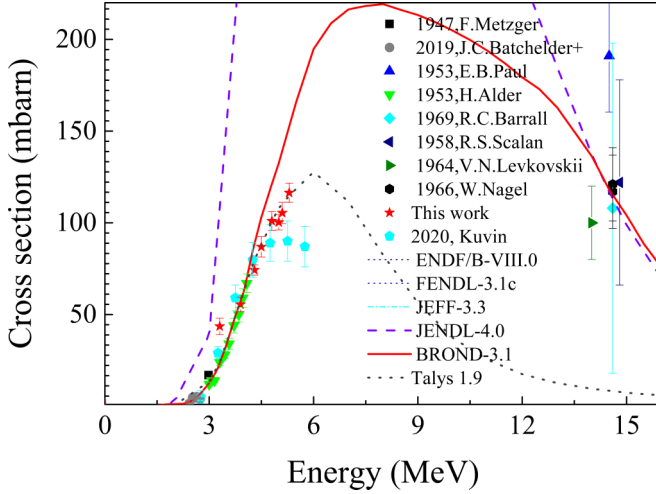


FIG. 8. Experimental and evaluated cross sections for the $^{35}\text{Cl}(n, \alpha_{\text{total}})^{32}\text{P}$ reaction and calculated results by TALYS-1.9.

JEFF-3.3 and BROND-3.1 in the neutron energy range of 3.9 to 4.3 MeV. At that time, our values of the (n, α) cross section for 4.8–5.3 MeV are lower than evaluations by the ENDF/B-VIII.0, FENDL-3.1c, JEFF-3.3, and BROND-3.1. It was seen that the JENDL-4.0 [20] gives considerably overestimated values for the $^{35}\text{Cl}(n, \alpha)^{32}\text{P}$ reaction cross sections in the investigated energy region. In addition, our experimental (n, α) cross sections are in good agreement with TALYS-1.9 calculations with adjusted optical model parameters (rvadjust a 0.95, avadjust a 0.95) excepting the 3.3 MeV where our datum is higher by a factor of ≈ 1.8 . Partial cross sections of two groups for discrete levels of the ^{32}P nucleus were obtained from the TALYS-1.9 calculation and compared with our experimental results shown in Table III and Fig. 9. The two groups $\alpha_{0,1,2}$ and $\alpha_{3,4,5}$ are well separated using the thin BaCl_2 target.

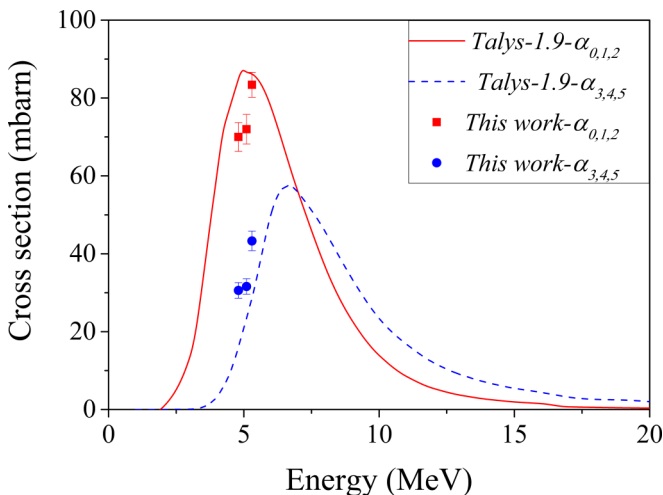


FIG. 9. Partial cross section of two groups for discrete levels of the ^{32}P nucleus.

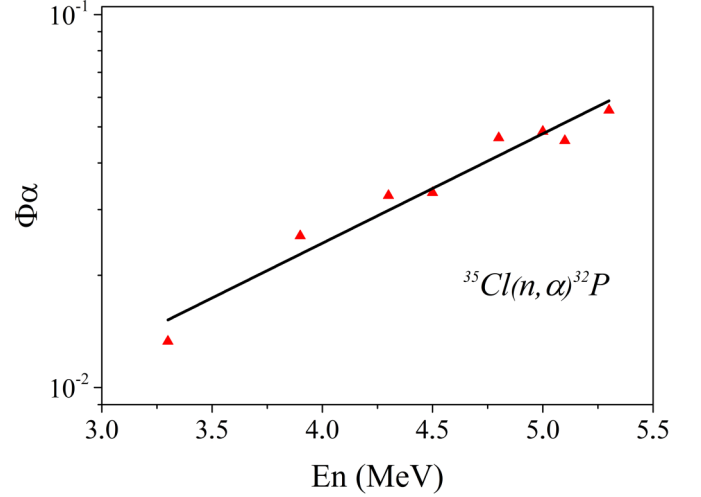


FIG. 10. Alpha cluster preformation factor vs neutron energy for the $^{35}\text{Cl}(n, \alpha)^{32}\text{P}$ reaction.

B. Alpha clustering in the $^{35}\text{Cl}(n, \alpha)^{32}\text{P}$ reaction

The preformation factor of an alpha cluster in a nucleus is defined as the probability of finding an alpha particle inside the parent nucleus. This factor refers to the clusterization of the alpha particle from four nucleons before the emission. Therefore, the value of this factor should be less than or equal to one [27]. In this work, we have tried to evaluate the alpha cluster preformation factor for the $^{35}\text{Cl}(n, \alpha)^{32}\text{P}$ reaction. The direct reaction mechanism can be used in the several MeV neutron energy range for medium-mass nuclei as a first approximation. Then, using the knock-on model the (n, α) cross section can be expressed as a two-stage process:

$$\sigma_{n,\alpha} = \Phi_{\alpha} \sigma_n^{\text{tot}}(^4\text{He}), \quad (4)$$

where Φ_{α} is the alpha cluster preformation factor and $\sigma_n^{\text{tot}}(^4\text{He})$ is the total neutron cross section for the ^4He (or α particle). From (4) the alpha cluster preformation factor can be obtained as

$$\Phi_{\alpha} = \frac{\sigma_{n,\alpha}}{\sigma_n^{\text{tot}}(^4\text{He})}. \quad (5)$$

Our results for the alpha clustering factor calculated by formula (5) are shown in Fig. 10.

In the calculations our experimental values of the total cross sections for ^{35}Cl (see Table II) and total neutron cross

TABLE III. Experimental results for $^{35}\text{Cl}(n, \alpha)^{32}\text{P}$ partial cross sections compared with TALYS-1.9 calculation using the adjusted input parameters.

Energy (MeV)	Cross sections (mbarn)			
	Experimental data		TALYS-1.9	
	$\sigma_{n,\alpha_{0,1,2}}$	$\sigma_{n,\alpha_{3,4,5}}$	$\sigma_{n,\alpha_{0,1,2}}$	$\sigma_{n,\alpha_{3,4,5}}$
4.8	70.0 ± 7.2	30.6 ± 3.4	84.9	16.0
5.1	72.0 ± 8.0	31.6 ± 3.8	86.7	23.4
5.3	83.4 ± 6.6	43.3 ± 4.4	86.2	28.7

sections for ^4He taken from ENDF/B-VIII.0 library [16] were utilized. As shown in Fig. 10, the alpha cluster preformation factor for the $^{35}\text{Cl}(n, \alpha)^{32}\text{P}$ reaction is almost linearly increased depending on the incident neutron energy from 3.3 to 5.3 MeV. In addition, it should be noted that values of the alpha cluster preformation factor are varied in the range of 1.33×10^{-2} to 5.55×10^{-2} , which are roughly close to those obtained in our previous works [28,29] using the statistical model for fast neutrons.

V. CONCLUSIONS

The $^{35}\text{Cl}(n, \alpha)^{32}\text{P}$ reaction cross sections were systematically measured with high accuracy at incident neutron energies of 3.3, 3.9, 4.3, 4.8, 5.0, 5.1, and 5.3 MeV. The obtained cross sections in the neutron energy range of 3.9 to 4.3 MeV are in agreement with evaluations by the ENDF/B-VIII.0, FENDL-3.1c, JEFF-3.3, and BROND-3.1, while for 4.8–5.3 MeV our experimental results are lower than the above-mentioned nuclear reaction data libraries. The total and

partial (n, α) cross sections are satisfactorily described by the TALYS-1.9 calculations with the adjusted optical model parameters.

Moreover, in the framework of the direct reaction mechanism, the alpha cluster preformation factor for the $^{35}\text{Cl}(n, \alpha)^{32}\text{P}$ reaction was determined using the knock-on model. The obtained values of the alpha clustering factor were ranged from 1.33×10^{-2} to 5.55×10^{-2} depending on neutron energy. These values of the alpha cluster preformation factor are roughly close to those obtained in our previous works using the statistical model.

ACKNOWLEDGMENTS

The authors are grateful to the operational team of the Van de Graaff accelerator EG-5 of the Frank Laboratory of Neutron Physics, JINR for kind cooperation. This work was supported by the LM2018108 project Van de Graaff Accelerator—a Tunable Source of Monoenergetic Neutrons and Light Ions of MEYS of the Czech Republic.

-
- [1] H. Kofuji, K. Komura, Y. Yamada, and M. Yamamoto, *J. Environ. Radioact.* **50**, 49 (2000).
- [2] T. Abram and S. Ion, *Energy Policy* **36**, 4323 (2008).
- [3] H. Alder, P. Huber, and W. Halg, *Helv. Phys. Acta* **26**, 349 (1953).
- [4] F. von Metzger, P. Huber, and F. Alder, *Helv. Phys. Acta* **20**, 236 (1947).
- [5] R. E. Lewis and T. A. Butler, *Nucl. Appl.* **2**, 102 (1966).
- [6] G. Pfrepper, *Isot. Environ. Health Stud.* **13**, 15 (1977).
- [7] S. Niese, *J. Kernenergie* **8**, 499 (1965).
- [8] E. Shikata, *J. Nucl. Sci. Technol.* **1**, 228 (1964).
- [9] J. C. Batchelder, S. A. Chong, J. Morrell, M. A. Unzueta, P. Adams, J. D. Bauer, T. Bailey, T. A. Becker, L. A. Bernstein, M. Fratoni, A. M. Hurst, J. James, A. M. Lewis, E. F. Matthews, M. Negus, D. Rutte, K. Song, K. Van Bibber, M. Wallace, and C. S. Waltz, *Phys. Rev. C* **99**, 044612 (2019).
- [10] R. C. Barrall, J. A. Holmes, and M. Silbergeld, Report: Air Force Spec. Weap. Center Kirtland A. F. B. Repts., AFWL-TR-68-134 (1969).
- [11] W. Nagel and A. H. W. Aten, *J. Nucl. Energy, Parts A/B* **20**, 475 (1966).
- [12] V. N. Levkovskiy, *J. Exp. Theor. Phys.* **18**, 213 (1964).
- [13] R. S. Scalan and R. W. Fink, *Nucl. Phys.* **9**, 334 (1958).
- [14] E. B. Paul and R. L. Clarke, *Can. J. Phys.* **31**, 267 (1953).
- [15] Experimental Nuclear Reaction Data (EXFOR), <http://www-nds.iaea.org/exfor/exfor.htm>.
- [16] Evaluated Nuclear Data File (ENDF), <http://www-nds.iaea.org/exfor/endl.htm>.
- [17] Neutron Evaluated Data Library BROND-3.1, <https://vant.ippe.ru/en/year2016/2/neutron-constants/1150-5.html>.
- [18] The Joint Evaluated Fission and Fusion File (JEFF-3.3), <https://www.oecd-nea.org/dbdata/jeff/jeff33/index.html>.
- [19] Fusion Evaluated Nuclear Data Library - FENDL-3.2, <https://www-nds.iaea.org/fendl>.
- [20] JENDL-4.0, <https://www.ndc.jaea.go.jp/jendl/j40/j40.html>.
- [21] S. A. Kuvina *et al.*, *Phys. Rev. C* **102**, 024623 (2020).
- [22] A. J. Koning, S. Hilaire, and M. C. Duijvestijn, *Proceedings of the International Conference on Nuclear Data for Science and Technology-ND2007* (Nice, France, 2007), p. 211.
- [23] A. J. Koning, S. Hilaire, and S. Goriely, *TALYS-1.9* (2017), <http://www.TALYS.eu/>
- [24] G. Zhang, Yu. M. Gledenov, G. Khuukhenkhuu, M. V. Sedysheva, P. J. Szalanski, J. Liu, H. Wu, X. Liu, J. Chen, and V. A. Stolupin, *Phys. Rev. C* **82**, 054619 (2010).
- [25] B. B. Rossi and H. H. Staub, *Ionization Chambers and Counters: Experimental Techniques* (McGraw-Hill, New York, 1949).
- [26] SRIM code, <http://www.srim.org>.
- [27] P. E. Hodgson, *The Uncertainty Principle and Foundations of Quantum Mechanics*, edited by W. C. Price and S. Chissick (Wiley, New York, 1977), Chap. 23.
- [28] G. Khuukhenkhuu, J. Munkhsaikhan, M. Odsuren *et al.*, in *Proceedings of the XXIV International Seminar on Interaction of Neutrons with Nuclei, Dubna, Russia, 2016* (JINR, Dubna, 2017), p. 166.
- [29] G. Khuukhenkhuu, M. Odsuren, Yu. M. Gledenov *et al.*, *Acta Phys. Pol. B* **49**, 325 (2018).